

# Self-Calibrating Microfabricated Iridium Oxide pH Electrode Array for Remote Monitoring

Susan Carroll and Richard P. Baldwin\*

Department of Chemistry, University of Louisville, Louisville, Kentucky 40292

The goal of this work is the development of microfabricated electrochemical sensing systems for environmental, industrial, and security applications requiring long-term unattended operation. The specific advantages of the microfabrication approach include the capability not only to miniaturize the size of the sensor platform but also to create an intelligent design including features such as redundant sensing electrodes, on-chip reference and auxiliary electrodes, and in situ electrode regeneration/calibration. The model system targeted here involves continuous pH monitoring in drinking water at solid-state iridium oxide electrodes. The microchips utilized consist of a flow-through silicon platform (1 cm × 1.2 cm) containing patterned gold electrodes onto which iridium oxide has been deposited electrochemically. To simulate drinking water detection scenarios, sensors are integrated into a flow system. Microfabricated designs include as many as 11 equivalent pH electrodes whose performance was evaluated for factors such as electrode-to-electrode reproducibility, long-term drift, and response to expected interfering agents. With on-chip voltage treatment, absolute potentials measured for an electrode array are within ±4 mV, with identical (±1 mV/pH unit) calibration slopes. This performance level is sustainable over weeks of usage.

Microfabrication techniques, developed primarily for the electronics and computer industries, have been employed for the past 10–15 years for the miniaturization of diverse analytical instrumentation. The most obvious characteristic of such microfabricated devices, their greatly diminished physical size, carries with it several distinct advantages including increased speed, reduced sample/reagent consumption, and the possibility of decreased costs through mass production. However, other perhaps more important benefits result from the capability to create a diverse collection of micrometer-sized structures able to carry out complex measurement operations, integrate them seamlessly onto a single platform, and then replicate this instrument on a large scale and with essentially absolute fidelity.

To date, most of this micro total analysis system or “lab on a chip” work has targeted biomedical applications such as DNA sequencing and analysis and high-throughput screening; and remarkable advances in these areas have occurred as a consequence.<sup>1,2</sup> However, it seems clear that microfabricated instrument

systems should have numerous unique applications in many other areas of analysis. One such application for which microfabrication seems particularly well suited is the development of “smart” sensors suitable for numerous environmental, industrial, and security applications requiring long-term, on-site measurements. Such experiments entail analyses that need to be carried out with minimal operator intervention (preferably none at all) but nevertheless with a reasonably high degree of reliability over extended periods of time.

Microfabrication is particularly well suited for electrochemically based sensors where the primary sensing element is a set of metallic electrodes, e.g., gold or platinum. Such materials are able to be patterned via photolithography and other conventional microfabrication techniques, and the resulting electrodes can be modified and optimized for specific applications by appropriate electrochemical postprocessing operations. As a consequence, the construction of customized electrode designs for specific applications and of complex but highly reproducible electrode systems can be readily realized. Finally, literally hundreds of electrode systems have already been reported for many important analytes. These include traditional potentiometric and voltammetric assay procedures as well as nonredox approaches involving conductimetry, ac impedance measurements, and the electrochemical microbalance. Therefore, in many cases, completely original electrode schemes do not need to be devised but rather these already well characterized electrodes may often only need to be adapted appropriately to the microfabricated format.

The specific goal of this work is to demonstrate the above concept by investigating simple ways in which the microfabrication approach can be used to make electrochemical sensors behave “more intelligently” and therefore provide improved performance for long-term remote monitoring applications. Specific features that have been incorporated onto the microfabricated sensor platform are (1) the inclusion of redundant sensing electrodes to function either as a back up when one sensor fails or as a way of verifying questionable results, (2) the integration of reference and auxiliary electrodes onto the sensor platform, and (3) the development of in situ electrode regeneration and calibration procedures.

The specific analytical problem that we consider here is the continuous pH monitoring of drinking water. Traditionally, the ideal sensor for pH monitoring has, of course, been the glass pH electrode. However, despite its attractive analytical capabilities with respect to selectivity and pH range, the glass electrode is rather poorly suited to conventional microfabrication techniques. A

\* To whom correspondence should be addressed. Phone: 502-852-5892. Fax: 502-852-8149. E-mail: rick.baldwin@louisville.edu.

(1) Dittrich, P. S.; Tachikawa, K.; Manz, A. *Anal. Chem.* **2006**, *78*, 3887–3907.

(2) West, J.; Becker, M.; Tombrink, S.; Manz, A. *Anal. Chem.* **2008**, *80*, 4403–4419.

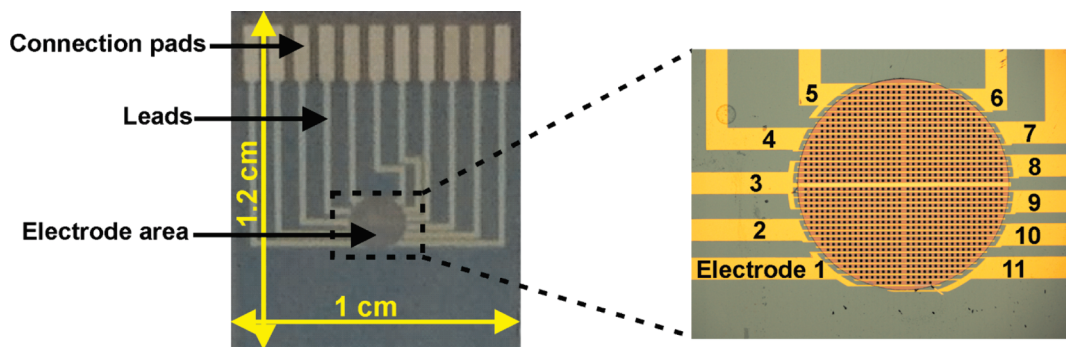


**Figure 1.** Photographs illustrating the entire microchip (left) and a close-up of the flow-through area containing the interdigitated working electrodes (right).

logical alternative is provided by metal oxide-based pH sensors that have been developed over the past 20–30 years and not only offer attractive pH measurement capabilities but also seem to be compatible in most respects with incorporation into microfabricated systems. A wide variety of metal oxides have been characterized and applied to pH measurement, including those involving Sb, Bi, Pd, Pt, Ir, Ru, Os, Ta, Rh, Ti, and Sn.<sup>3–6</sup> Although several of these oxide systems may be suitable, iridium oxide ( $\text{IrO}_x$ ) was selected for use in this study because of its attractive stability and relative freedom from interferences. Most important,  $\text{IrO}_x$  can be prepared electrochemically and deposited onto a variety of conducting substrates by electro-oxidation/reduction of appropriate Ir complexes.<sup>7–17</sup> This characteristic makes  $\text{IrO}_x$ -based sensors well suited for use in microfabricated devices in which noble metal substrates have been patterned photolithographically and then modified as needed with the pH-sensitive  $\text{IrO}_x$  film.

Previously, there have been a few instances reported of microfabricated metal oxide sensor systems. For example, Marzouk et al. described the design and performance of implantable  $\text{IrO}_x$ -coated Pt electrodes for measurement of extracellular pH associated with myocardial ischemia.<sup>11</sup> Subsequently, Baudenbacher's group used similar procedures to place  $\text{IrO}_x$  electrodes on microfluidic chips for monitoring pH changes related to growth and activity of cell cultures.<sup>8,9</sup> In all of these cases, the

microfabricated electrodes exhibited excellent analytical performance, especially with respect to pH range, response time, and lack of drift. However, these studies took advantage primarily of the small electrode dimensions and precise electrode orientation made possible by microfabrication and were not concerned with the use of this methodology to create electrode arrays or systems that offered the increased reliability and independence required for remote monitoring applications. A promising approach in this direction was suggested by Vonau et al. who proposed the integration of an  $\text{RuO}_2$ -based pH electrode with  $\text{Cl}^-$ ,  $\text{NO}_3^-$ , and  $\text{NH}_4^+$  ion selective electrodes to create a “smart card” that might be used on-site for routine analysis of samples such as drinking water.<sup>18</sup> However, despite the intriguing nature of the study, only minimal information regarding the fabrication processes employed and almost no performance data were provided.

In this work, we report the construction of a microfabricated platform specifically designed for pH measurement and incorporating features to facilitate subsequent applications targeting independent on-site analysis. The resulting microchips (Figure 1) consisted of a flow-through silicon platform containing a patterned array of gold electrodes which were converted to pH electrodes via postprocessing electrodeposition of an  $\text{IrO}_x$  coating. The designs included as many as 11 equivalent pH sensors whose performance was evaluated for factors such as electrode-to-electrode reproducibility, short- and long-term drift, and the effectiveness of on-chip calibration procedures.

## EXPERIMENTAL SECTION

**Materials.** Universal pH buffers (4, 7, and 10), oxalic acid, and potassium carbonate (anhydrous) were purchased from VWR International (Batavia, IL). Iridium(IV) chloride hydrated and platinum wire (99.95%) were obtained from Strem Chemicals, Inc. (Newburyport, MA). All chemicals were used without further purification. Phosphate buffer solutions (0.2 M, pH ~6.6) and other solutions were prepared as needed using deionized (DI) water.

**Chip Fabrication.** Only a brief overview of the microfabrication process will be given here, since the production procedure is being reported separately. In general, an oxidized 4 in. silicon wafer was employed as the substrate onto which various gold electrode arrays were patterned via photolithography. First, the

- (3) Ives, D. J. G.; Janz, G. J. *Reference Electrodes*; Academic Press: New York, 1961.
- (4) Einerhand, R. E. F.; Visscher, W. H. M.; Barendrecht, E. *Electrochim. Acta* **1989**, *34*, 345–353.
- (5) Liu, C. C.; Bocchicchio, B. C.; Overmyer, P. A.; Neuman, M. R. *Science* **1980**, *207*, 188–189.
- (6) Fog, A.; Buck, R. P. *Sens. Actuators* **1984**, *5*, 137–146.
- (7) Yamanaka, K. *Jpn. J. Appl. Phys., Part 1* **1989**, *28*, 632–637.
- (8) Ges, I. A.; Ivanov, B. L.; Schaffer, D. K.; Lima, E. A.; Werdich, A. A.; Baudenbacher, F. J. *Biosens. Bioelectron.* **2005**, *21*, 248–256.
- (9) Ges, I. A.; Ivanov, B. L.; Werdich, A. A.; Baudenbacher, F. J. *Biosens. Bioelectron.* **2007**, *22*, 1303–1310.
- (10) Marzouk, S. A. M. *Anal. Chem.* **2003**, *75*, 1258–1266.
- (11) Marzouk, S. A. M.; Ufer, S.; Buck, R. P.; Johnson, T. A.; Dunlap, L. A.; Cascio, W. E. *Anal. Chem.* **1998**, *70*, 5054–5061.
- (12) Petit, M. A.; Plichon, V. J. *Electroanal. Chem.* **1998**, *444*, 247–252.
- (13) Zhang, J. M.; Lin, C. J.; Feng, Z. D.; Tian, Z. W. *J. Electroanal. Chem.* **1998**, *452*, 235–240.
- (14) Meyer, R. D.; Cogan, S. E.; Nguyen, T. H.; Rauh, R. D. *IEEE T. Neur. Sys. Reh.* **2001**, *9*, 2–11.
- (15) Elsen, H. A.; Monson, C. F.; Majda, M. J. *Electrochem. Soc.* **2009**, *156*, F1–F6.
- (16) Chen, Y. J.; Taylor, P. L.; Scherson, D. J. *Electrochem. Soc.* **2009**, *156*, F14–F21.
- (17) Bezbaruah, A. N.; Zhang, T. C. *Anal. Chem.* **2002**, *74*, 5726–5733.

- (18) Vonau, W.; Enseleit, U.; Gerlach, F.; Herrmann, S. *Electrochim. Acta* **2004**, *49*, 3745–3750.

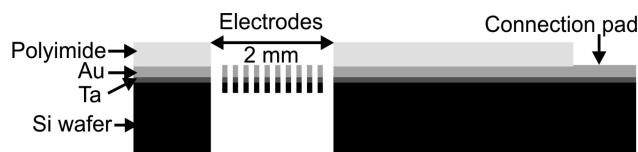


**Figure 2.** Schematic side view of the microchip illustrating the arrangement of the different material layers.

gold electrodes (with a tantalum adhesion layer) were created by sputtering to a thickness of approximately 250 nm. Next, a polyimide layer, approximately 3  $\mu\text{m}$  thick, was created to define the exposed electrode area and to insulate the electrical leads from the electrode area to the connection pads. Holes extending through the wafer for flow-through operation were created in two steps: reactive ion etching of the electrode-side of the chip (after protection of the polyimide with a layer of aluminum) and deep reactive ion etching of the backside of the chip. A cross-sectional view of the resulting structure is shown in Figure 2. In all, four separate photolithography steps were required: to pattern the Au electrodes, the polyimide coating, and the front- and backside perforations.

Specific device designs ranged from a simple microchip containing a single electrode to one containing 11 interdigitated electrodes. This 11-electrode array, which was the design mainly utilized in this study, is depicted in Figure 1. A total of 38 finger electrodes with a width of 15  $\mu\text{m}$  and varying in lengths are contained to the 2 mm diameter electrode area. All 11 electrodes have different surface areas ranging from the smallest area (electrode no. 6) of 0.055  $\text{mm}^2$  to the largest (electrode no. 3) of 0.196  $\text{mm}^2$ . This area is perforated (hole size 25  $\times$  25  $\mu\text{m}$ ) enabling the chip to be incorporated into a flow through system to simulate drinking water detection scenarios.

**Iridium Deposition Solution.** The electrochemical iridium oxide deposition solution was prepared after a protocol first described by Yamanaka<sup>7</sup> and later utilized and modified by others.<sup>8–13</sup> A total of 75 mg of iridium(IV) chloride was dissolved in 50 mL of DI water and stirred for 15 minutes. Next, 0.5 mL of 30%  $\text{H}_2\text{O}_2$  was added and stirred for 10 more minutes, and then 250 mg of oxalic acid was added with another 10 min stirring period. The resulting solution was slowly adjusted to pH 10.5 with anhydrous potassium carbonate and left to stabilize at room temperature for 2 days. Afterwards, the iridium solution was stored in the refrigerator and could be used for several weeks.

A pulsed potential deposition method was found to work best to deposit  $\text{IrO}_x$  electrochemically onto the microfabricated gold electrodes.<sup>14</sup> The  $\text{IrO}_x$  film was formed by potential pulsing between 0.0 V and 0.55 V (versus Ag/AgCl reference and a Pt wire counter electrode) at a 2 Hz frequency for 2400 cycles (40 min). When not in use, the  $\text{IrO}_x$  electrodes were stored in pH 7 buffer.

**Instrumentation.** Cyclic voltammograms (CVs) and constant potential treatments were carried out using a Bioanalytical Systems CV-50W voltammetric analyzer. Pulsed potential iridium depositions were accomplished employing a CHI 660A Electrochemical Workstation. All voltammetric experiments used a three-electrode cell with Ag/AgCl (3 M NaCl) reference and Pt wire counter electrodes.

All pH measurements were performed with a Thermo Orion model 320 potentiometer and verified by a commercially available glass electrode. A custom fabricated Delrin flow-through cell containing an access hole for a commercial Ag/AgCl reference electrode (1.9 cm downstream of the electrode area) was utilized to conduct flow through experiments with buffer solutions and drinking water. Solution flow was gravity driven, and the flow rate was determined by adjusting the height of the solution reservoir above the cell. Two water reservoirs were connected to the flow through system enabling a fast switch from one solution to another.

## RESULTS AND DISCUSSION

**Iridium Oxide Deposition Process.** Over the past 20–25 years, many different groups have explored various strategies for preparing  $\text{IrO}_x$  deposits suitable for use as pH sensors, reference electrodes, and neural stimulation electrodes. In general, these fabrication methods can be grouped into four principal classifications: thermal treatment/decomposition of iridium or iridium compounds, sputtering from an iridium target onto the surface of a suitable substrate, electrochemical oxidation of an iridium substrate, and electrodeposition of  $\text{IrO}_x$  onto a substrate surface from a solution containing a suitable iridium complex. The resulting  $\text{IrO}_x$  films, though all suitable for pH sensing, have been shown to exhibit a wide variation in pH response (i.e., sensitivity, drift, etc.) depending on whether the  $\text{IrO}_x$  deposit is considered to be “anhydrous” or “hydrated”. The former tends to result from the thermal and sputter-coating fabrication methods while the latter is usually associated with the electrochemical-based methods. A useful summary can be found in Madou’s 2001 review.<sup>19</sup> For our intended applications, involving microfabricated pH sensing devices, the most attractive  $\text{IrO}_x$  formation approach seemed to be that utilizing Ir electrodeposition. First and foremost, this procedure was the most flexible, allowing the use of completely conventional microfabrication techniques to create the device platform and then the application of relatively straightforward electrochemical postprocessing to convert selected electrodes to  $\text{IrO}_x$  pH sensors. In addition, the electrodeposition also avoided high temperatures during the fabrication process and the need for a dedicated Ir sputtering target.

However, even with the electrodeposition approach to  $\text{IrO}_x$  film formation, there is still a wide variety of specific experimental procedures that have been reported. As summarized recently by Majda,<sup>15</sup> these variations center around (1) the nature of the Ir solution used and whether Ir oxalate complexes are employed or not and (2) the nature of the electrochemical procedure, constant current vs constant potential vs pulsed or scanned potential, used to carry out the deposition.

The former issue proved to be straightforward, and oxalate-based solutions analogous to that described initially by Yamanaka<sup>7</sup> were always employed in this study. The behavior reported previously, namely, a 2 day induction period required for formation of the stable blue deposition solution, was observed consistently here, and the resulting  $\text{IrO}_x$  electrodes consistently exhibited the expected pH activity. However, the latter question concerning the electrochemistry operation was much more problem-

(19) Yao, S.; Wang, M.; Madou, M. *J. Electrochem. Soc.* **2001**, *148*, H29–H36.



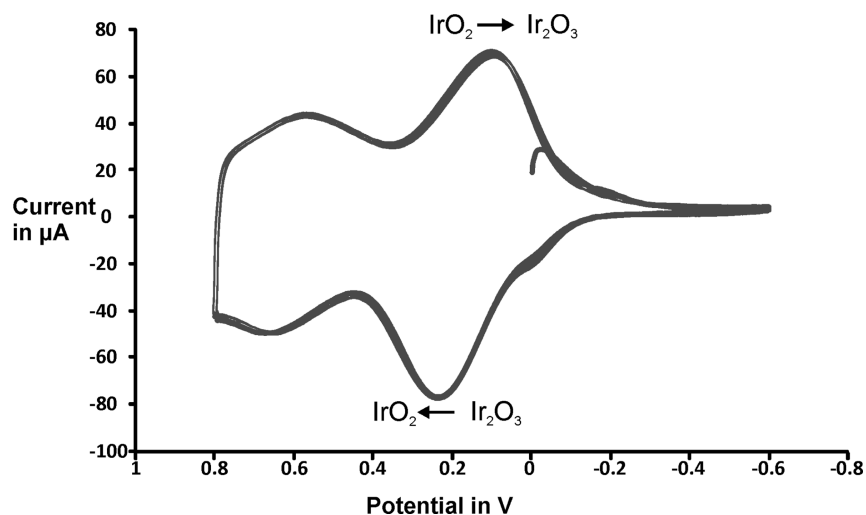


**Figure 3.** Cyclic voltammogram of an iridium oxide-coated Au electrode performed in pH 6.6 PBS at a scan rate of 50 mV/s.

atic; and during the course of this work, nearly all of the earlier procedures were investigated. In particular, we found that although the constant current or galvanostatic approach<sup>7–12</sup> appeared to work acceptably for  $\text{IrO}_x$  deposition onto either carbon or platinum substrates, it did not yield uniform films on gold electrodes, either for large Au disk electrodes obtained commercially or for our smaller microfabricated Au electrodes. Rather, with Au, visual inspection showed that the deposited  $\text{IrO}_x$  films usually varied greatly in color and thickness across the electrode surface and that the surface coverage of the underlying Au was often incomplete. In addition, when used to monitor pH,  $\text{IrO}_x$  films deposited onto Au electrodes regularly exhibited unacceptable short-term and long-term drifts in the observed potential readings and were sometimes prone to delamination from the Au substrate. Similar problems were also encountered with Au when the alternative constant potential approach<sup>13</sup> was employed.

Fortunately, greatly improved  $\text{IrO}_x$  films were obtained after switching to a pulsed potential electrodeposition strategy, similar to that developed by Meyer et al.<sup>14</sup> for preparing  $\text{IrO}_x$  coatings for implanted electrodes used for electrostimulation treatment of muscle and nerve tissue. In this protocol, the  $\text{IrO}_x$  deposit is grown by repeated application of brief oxidizing potentials, with the layer thickness determined by the length of time for which the potential pulsing was allowed to continue. The specific protocol that proved optimum for our microfabricated Au electrodes, pulsing between 0.0 V and +0.55 V (vs Ag/AgCl) for 40 min, was found to produce thick, visually uniform, and reproducible  $\text{IrO}_x$  deposits that were chemically and mechanically stable in buffer solutions for months and exhibited only very small drifts in both absolute potential and pH sensitivity. In addition to visual inspection, CV was also used to examine the nature of the electrodeposited  $\text{IrO}_x$  and any qualitative or quantitative changes that may have occurred over time. As shown in Figure 3, a typical CV, run in pH 6.6 phosphate buffer for a freshly prepared  $\text{IrO}_x$ -coated Au electrode, contained the expected  $\text{Ir}^{3+}/\text{Ir}^{4+}$  oxidation peak at ~250 mV and the corresponding reduction peak at ~50 mV, and scanning across the oxidation wave caused the appearance of the coating to change from colorless ( $\text{Ir}_2\text{O}_3$ ) to bright blue ( $\text{IrO}_2$ ). This CV

behavior is identical to what has been described for the  $\text{IrO}_x$  in numerous earlier studies.<sup>10–12,14,16,20</sup>

The optimization of the  $\text{IrO}_x$  deposition procedure described above was carried out primarily using commercial macrosized Au disk electrodes. Therefore, once the optimization was completed, the next step was to establish how effectively this procedure could be extended to microfabricated Au electrode arrays. Since our overall goal was to obtain a smart sensor that can operate in remote sensing settings with little or no external assistance, one strategy was to incorporate several redundant sensing electrodes on a single microchip platform. With this objective in mind,  $\text{IrO}_x$  was deposited onto a chip (see Figure 1) that contained 11 independent Au microelectrodes. For this procedure, all the electrodes were connected together; and the  $\text{IrO}_x$  was deposited onto all 11 in a single operation using the same experimental conditions developed above for conventional Au electrodes. Subsequently, the 11 electrodes were disconnected from one another, and the pH-sensing performance of each of the individual electrodes was evaluated and compared.

The results of this operation are summarized in Table 1. In general, the  $\text{IrO}_x$  deposition proceeded on the microchip exactly as expected, with visual and microscopic inspection indicating a complete and uniform coating of all 11 electrodes. In addition, CVs run separately on each electrode were all identical in appearance to that shown in Figure 3 for a Au/ $\text{IrO}_x$  macroelectrode and confirmed further that the deposition process had proceeded similarly. Because the individual microelectrodes were all different in size for this chip design, the magnitude of the CV currents was not identical for each but rather was determined by the electrode area. Of course, for the potentiometric pH measurements of interest here, these differences in electrode size had no influence on electrode performance. Most important, when examined in pH 4, 7, and 10 buffers, all 11 exhibited similar potential response, with slopes ranging from –63.8 to –69.5 mV/pH. This corresponds well to the pH behavior reported previously for hydrated  $\text{IrO}_x$  films.<sup>19</sup> Finally,

(20) Burke, L. D.; Mulcahy, J. K.; Whelan, D. P. *J. Electroanal. Chem.* **1984**, *163*, 117–128.

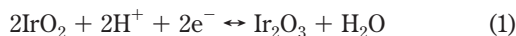
**Table 1. Absolute Potential Responses and Sensitivities before (A) and after (B) Treatment**

	electrode										
	1	2	4	5	6	7	8	9	10	11	range
(A) Without Treatment											
pH 10 (mV)	97	81	62	60	65	51	14	32	24	75	83
pH 7 (mV)	310	297	274	272	274	262	222	241	226	271	88
pH 4 (mV)	505	498	470	473	470	458	422	440	419	458	86
slope	-68.0	-69.5	-68.0	-68.8	-67.5	-67.8	-68.0	-68.0	-65.8	-63.8	5.7 mV/pH
(B) After 200 mV Treatment											
pH 10 (mV)	-3	-8	-7	-7	-9	-14	-12	-6	-13	-10	11
pH 7 (mV)	205	205	206	206	201	197	201	206	199	199	9
pH 4 (mV)	408	411	414	418	407	398	407	415	404	401	20
slope	-68.5	-69.8	-70.2	-70.8	-69.3	-68.7	-69.8	-70.2	-69.5	-68.5	2.3 mV/pH

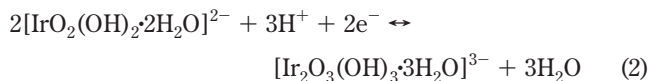
when examined over a long period of time, the Au/IrO<sub>x</sub> electrodes proved quite durable. The particular microchip that gave rise to the data in Table 1 was used on a daily basis for at least 4 months during which time hundreds of pH measurements were performed.

**On-Chip pH Calibration.** For routine pH monitoring, the performance shown in Table 1A would probably prove acceptable. However, for the remote monitoring applications envisioned here, where conventional calibration with pH buffers would not be convenient, it is imperative that any single electrode behaves exactly the same over its entire lifetime and that drift in response over time, whether due to electrode aging, temperature, or other factors, should either be insignificant in extent or easily correctable. In addition, if any single electrode, upon malfunction, is to be replaced by another residing on the microchip, it is also essential that all redundant electrodes behave identically to one another. Unfortunately, Table 1A shows that this was not the case as the electrode-to-electrode variation in absolute potential readings seen for the pH 4, 7, and 10 buffers was 86, 88, and 83 mV, respectively, and electrode-to-electrode variation in the calibration slope over this pH range was 5.7 mV/pH.

A practically useful solution to this problem was provided by the fact that the potentiometric pH response mechanism for the IrO<sub>x</sub> electrode is fundamentally different from that of traditional ion selective electrodes. For most such systems (e.g., the glass pH electrode), the potential is generated at the solution/electrode interface and depends primarily on the solution-phase activities of the relevant ions. However, in the case of metal oxide electrodes, the pH response not only depends on the H<sup>+</sup> activity but also on the oxidation state of the iridium film, with the suggested working reactions typically given as



for an anhydrous IrO<sub>x</sub> electrode and



for the hydrated IrO<sub>x</sub> system. Thus, for electrodes prepared via different methodologies, the Nernstian response slopes can range between 59 and 88.5 mV/pH; and electrodes such as ours that exhibit intermediate slopes (60–70 mV/pH) are generally assumed to have a mixed IrO<sub>x</sub> composition and be

operating under a correspondingly mixed reaction mechanism.<sup>20</sup> Further, consideration of the related Nernst equations, e.g.,

$$E = E^0 - 2.3RT/2F \log[\text{Ir}_2\text{O}_3]/[\text{IrO}_2]^2[\text{H}^+]^2 \quad (3)$$

and

$$E = E^0 - 2.3RT/2F \log[\text{Ir}_2\text{O}_3]/[\text{IrO}_2]^2[\text{H}^+]^3 \quad (4)$$

suggests that any variation in the Ir<sup>3+</sup>/Ir<sup>4+</sup> ratio should also have a predictable effect on the pH response. In fact, this latter consideration has frequently been invoked to explain variations in potentials observed not only for IrO<sub>x</sub> electrodes prepared by different methods but also for IrO<sub>x</sub> electrodes as they age or are exposed to redox agents during operation. For example, newly prepared electrodes have been reported to vary in their potential response up to 100 mV,<sup>21</sup> and deliberate exposure to redox agents such as Fe(CN)<sub>6</sub><sup>3-/4-</sup> have been shown to eliminate pH sensitivity entirely.<sup>17</sup>

The most important implication of this analysis is that, just as variations in the Ir<sup>3+</sup>/Ir<sup>4+</sup> ratio during usage may cause an electrode's pH response to vary, restoration of an electrode's initial redox state might restore it to its original activity. In fact, as early as 1992, Hitchman, working with thermally prepared anhydrous IrO<sub>x</sub>, showed that both the absolute starting potential reading and the overall stability of a series of electrodes could be dramatically improved after application of an appropriate potential for a 5–30 min period.<sup>21</sup> By this approach, the variation in response of four IrO<sub>x</sub> electrodes whose starting potentials varied over nearly 100 mV was made to converge to just a 10 mV range. Despite the obvious utility of this technique, it seems to have been largely overlooked since its initial report and we have been able to find no subsequent application of analogous potential pretreatment schemes in the production or use of metal oxide pH electrodes. Nevertheless, for our microfabricated electrode arrays, Hitchman's electrochemical treatment approach presented a very attractive method both to improve interelectrode reproducibility and perhaps to allow a simple and effective way to "recalibrate" pH electrodes in the field without the need for standard buffers.

Accordingly, the same IrO<sub>x</sub> electrodes whose response is shown in Table 1, part A were subjected to a potential treatment that consisted of immersion in pH 7 buffer and application of 200

(21) Hitchman, M. L.; Ramanathan, S. *Talanta* **1992**, *39*, 137–144.

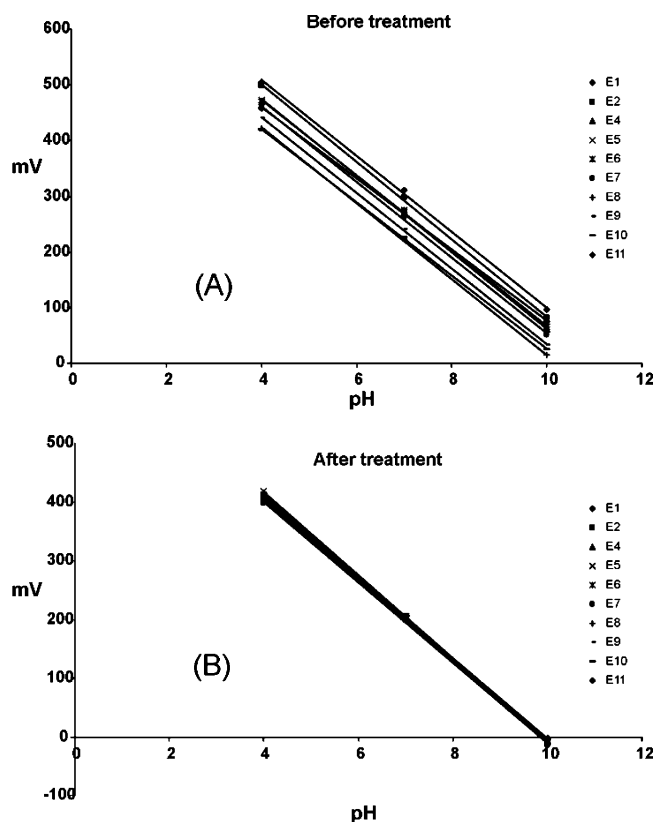


**Figure 4.** Calibration curves of the IrO<sub>x</sub> electrodes in pH 4, 7, and 10 buffer solutions before (A) and after (B) potential treatment.

mV (vs Ag/AgCl) for 3 min. (At the time of this treatment, the microchip had already undergone over 3 months of routine testing and the electrodes had already shown clear deviations from their original potentials and slopes.) This particular potential, which was reasonably close to the electrodes' original potential reading for pH 7, was chosen because, based on the IrO<sub>x</sub> CV in Figure 3, it should ensure significant amounts of both Ir<sup>3+</sup> and Ir<sup>4+</sup> oxidation states. Table 1, part B shows that, after this 3 min treatment, the absolute potential readings obtained in pH buffers converged dramatically. Compared to the earlier 80–90 mV differences, the interelectrode responses were reduced to 10–20 mV ( $\pm 4$  mV). This corresponds to a difference in pH of 1.4 and 0.29, respectively. In addition, the variation in the calibration sensitivity was also significantly reduced, with the range of slopes decreased from 5.7 mV/pH before the potential treatment to 2.3 mV/pH ( $\pm 1$  mV/pH unit) following it. The effect of the 200 mV treatment is perhaps best illustrated in Figure 4 where the overall pH response is shown graphically both before and after the procedure.

**Rationale.** The apparent explanation for the success of the 200 mV treatment procedure is that, during preparation or during extended usage, the Ir<sup>3+</sup>/Ir<sup>4+</sup> composition of the IrO<sub>x</sub> electrode can vary and that, as suggested by Hitchman,<sup>21</sup> the application of an external potential provides a convenient mechanism for both restoring the composition of an individual electrode to its initial state and bringing that of different electrodes into a close degree of convergence. Several observations made during this study provide qualitative support for this explanation. For example, we noted early on distinct differences in pH behavior for the electrodes depending on the ending potential for the

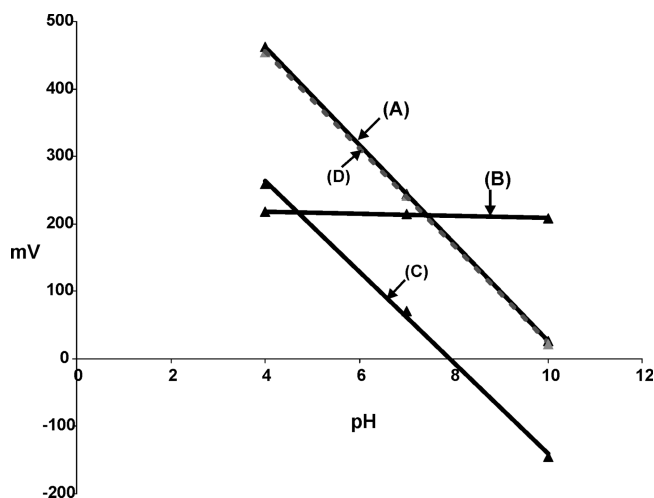


**Figure 5.** Calibration curves of a freshly prepared IrO<sub>x</sub> electrode in pH 4, 7, and 10 buffer solutions. Trace A shows the original pH response. Trace B was acquired after addition of 0.01 M ferri-/ferrocyanide to the buffer solutions. Trace C is the response curve after removal of the ferri-/ferrocyanide, and trace D is the restored pH response after a 3 min treatment in pH 7 buffer (gray dotted line).

IrO<sub>x</sub> deposition which could be either reducing (0.0 V vs Ag/AgCl) or oxidizing (+0.55 V) in view of the pulsed potential electrodeposition procedure employed. Next, it is well-known that Ir<sup>4+</sup> oxide species tend to be blue in color. As our IrO<sub>x</sub> electrodes aged during use, they gradually lost their initial blue color and took on a largely colorless appearance indicative of Ir<sup>3+</sup>. Finally, we electrodeposited IrO<sub>x</sub> onto an optically transparent indium/tin oxide slide and then observed its absorbance *in situ* as a function of applied potential. Potentials ranging from 600 to –200 mV were applied in 100 mV increments in pH 7 buffer, and absorption spectra were taken from 400 to 800 nm. At the initial 600 mV potential, the IrO<sub>x</sub> deposit was blue in color, with a maximum absorbance at 635 nm. Almost no changes in the spectrum were observed down to 400 mV, but at 300 mV the 635 nm absorbance started to decrease. This suggested that, at the 200 mV pretreatment potential, some of the Ir<sup>4+</sup> was already converted to the colorless Ir<sup>3+</sup> form and that a mixture of the two redox states is necessary to obtain an ideally functioning pH electrode.

One of the strengths of IrO<sub>x</sub> in pH sensing is its relative freedom from interference from many simple ions and complexing agents.<sup>6,11,17</sup> However, like most metal oxide systems, IrO<sub>x</sub> response is known to be particularly sensitive to the presence of redox species.<sup>6,17</sup> Accordingly, as a final test of the above treatment procedure to provide an effective calibration approach, exposure of the IrO<sub>x</sub> to redox agents was also investigated. In particular, the ferri-/ferrocyanide couple was selected as the interfering agent of choice because Bezbaruah and Zhang<sup>17</sup> recently showed that the pH sensitivity of IrO<sub>x</sub> can be blocked completely by the presence of this redox couple. Our experiments, shown in Figure 5, confirmed the severity of this problem. While a freshly prepared IrO<sub>x</sub> electrode exhibited the expected pH response for pH 4–10 buffers (Figure 5, trace A), addition of 0.01 M ferri-/ferrocyanide to the buffers virtually eliminated the effect of pH on the observed electrode potential (trace B). While removal of the ferri-/ferrocyanide and return of

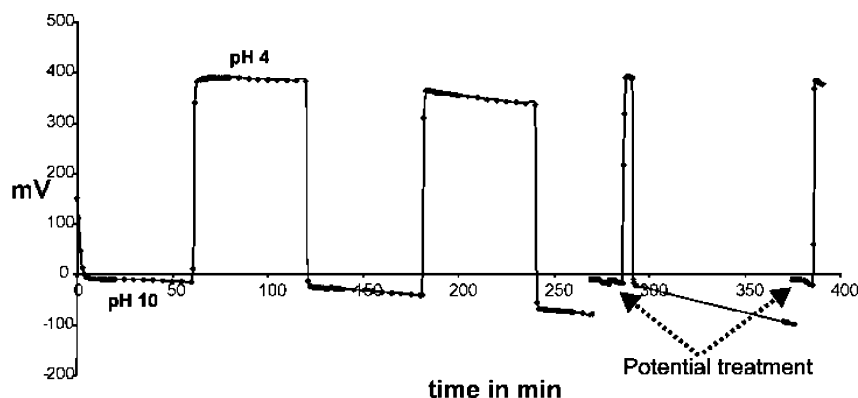


**Figure 6.** Potential response of the microchip containing  $\text{IrO}_x$  electrode incorporated into a flow system. Buffer solutions (pH 4 and 10) were alternately passed through the chip; after 275 min, a potential treatment of  $-14$  mV was applied to the working electrode to correct for negative drift ( $\sim 60$  mV).

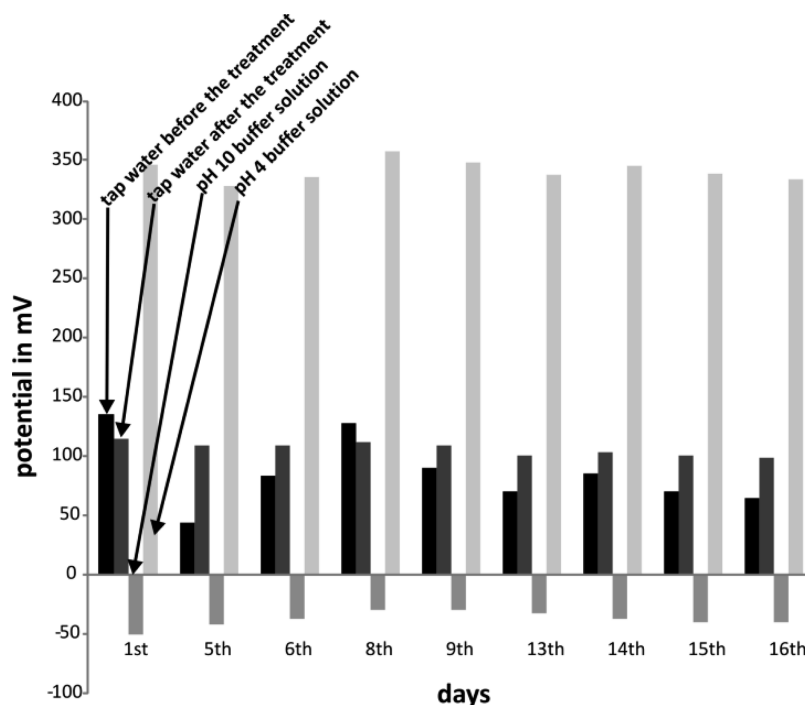


**Figure 7.** Potential responses of the microchip incorporated into a flow-through system for 16 days in tap water. Potential treatment of 115 mV (6 min) was applied, and the electrode pH responsive was verified by passing pH 4 and 10 buffer solutions through the chip.

the electrode to pristine buffer solutions did allow its general pH sensitivity to be restored, the new potential readings were displaced by more than 150 mV from their initial values (trace C). In practice, such a displacement, which is consistent with a net reduction of the Ir deposit, would have a serious effect on the measurement; and without recalibration, the new pH readings would be changed by as much as 2 pH units. However, as can be seen from trace D, application of the above pretreatment procedure (i.e., 3 min in pH 7 buffer) returned the electrode's pH response nearly exactly to its starting state. This experiment showed obvious promise for the possibility of on-site sensor recalibration after exposure to oxidizing and/or reducing agents that might be encountered in drinking water analysis.

**Applications in Flow Systems.** Up to this point, all pH measurements and pretreatments had been carried out in bulk solution by simply immersing the  $\text{IrO}_x$  electrodes into an unstirred buffer/analyte solution. In order to simulate actual water quality

testing scenarios, the microchip was integrated into a flow-through system which contained a downstream commercial Ag/AgCl reference electrode. The chip utilized for the flow-through experiments described below contained a six-segmented electrode array. One of the electrodes was coated with  $\text{IrO}_x$  for pH sensing, and the others were kept as bare Au electrodes, thereby enabling them to function as a counter electrode for any desired pretreatment experiments. Initial experiments employed standard pH buffers since, unlike actual tap water, these have a fixed and well-known composition with respect to ionic strength, dissolved organics, etc.

Typical flow-cell results are shown in Figure 6. In this experiment, the potential of an  $\text{IrO}_x$  was monitored over time as pH 10 and pH 4 buffers were alternately passed through the cell. As can be seen, although the observed potential readings were relatively stable initially, a substantial negative drift ensued that after 4 h amounted to approximately 60 mV. Other than

this drift, the IrO<sub>x</sub> electrode continued to respond rapidly to changes in the buffer pH. Subsequently, a potentiostatic treatment, consisting of holding the electrode at -14 mV for 6 min, was applied. (Note that a different treatment potential from that used earlier was employed here because, unlike the previously described +200 mV treatments that were carried out in pH 7 buffer, the treatment medium in this study was pH 10 buffer.) Clearly, this procedure was again successful in restoring that electrode's original response. Moreover, although the electrode output continued to drift after the treatment, the protocol could be repeated at will to restore the electrode response and make accurate pH readings possible. Only two treatment cycles are shown in the figure, but we found that the procedure remained effective for numerous pretreatments over periods of weeks.

Finally, the sensor performance under more realistic conditions was examined by obtaining longer-term pH measurements made directly on municipal (Louisville, KY) tap water. As above, these measurements were made by continuously flowing the water sample through the microchip for the entire duration of the experiment; and the sole pretreatment of the tap water consisted of filtration to remove particulates and prevent possible clogging of the perforated electrode area during such long time use. Throughout the course of the reported experiment, the pH of the specific water sample employed was 8.05 as determined at the outset and verified daily with a standard glass electrode.

Figure 7 summarizes the chip performance obtained over a 16-day measurement period. For each set of pH measurements shown, the initial potential reading corresponded to the potential of the IrO<sub>x</sub> electrode on that day without any treatment or modification. Clearly, there was a significant and mostly random drift in this potential reading from day to day. Subsequently, the electrode was treated by holding it at +115 mV for a 6 min period and then allowed to equilibrate for 5 min. The potential values, remeasured at this point, showed a maximum deviation of only 16 mV ( $\pm 5.3$  mV) over the entire course of the experiment. This corresponds to a maximum difference in pH readings of 0.24 ( $\pm 0.08$ ). In order to confirm that the electrode's overall pH response was still in place, the tap water was briefly replaced by pH 10 and pH 4 buffers, and potential readings were made in each of the media. Despite a relatively small random drift, the IrO<sub>x</sub> electrode remained well calibrated over the 16 day test period.

## CONCLUSIONS

In this work, we have investigated a few simple strategies, made possible by microfabrication methodologies, for improving sensor performance for on-site and especially unattended operation. Specifically in the case of pH measurement, arrays of microfabricated Au electrodes coated with IrO<sub>x</sub> films were shown to perform effectively for drinking water samples from municipal treatment facilities. Perhaps most important, a simple potentiostatic calibration procedure, requiring no external buffer solutions, was shown to be highly effective both for standardizing the absolute potential response of all the individual electrodes in the array and for restoring the potential response of a single electrode over an extended period of time. These represent a few examples illustrating simple ways in which microfabrication can be employed to allow instrumentation to operate at a more "intelligent" and independent level.

Although automated monitoring of pH alone may be important for some applications, integration of additional sensing functions would be necessary in order to achieve a practical device suitable for general surveillance of drinking water quality. For example, inclusion of sensors for other parameters such as conductivity, redox potential, and disinfectant level would certainly increase the available analytical information to a very useful level. Interestingly, not only do electrochemical approaches appear to be well suited to the design of sensors for all of these parameters, but also their actual construction and miniaturization seem highly amenable to conventional microfabrication techniques. Therefore, we expect that there will be rapid progress in the development of smart microfabricated sensors for routine monitoring of water quality. In addition, in view of the innumerable practical applications of electroanalysis that are already well-known, it seems likely that the approach can be extended to very many important measurement situations.

## ACKNOWLEDGMENT

This work was supported by the NSF Grant BES-0529140 and was greatly appreciated. Additionally, we would like to acknowledge Michael M. Martin for his microchip fabrication work.

Received for review September 9, 2009. Accepted December 20, 2009.

AC9020374